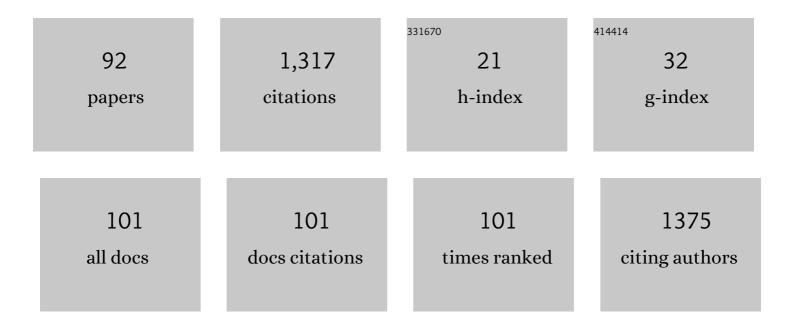
List of Publications by Year in descending order

Source: https://exaly.com/author-pdf/7276771/publications.pdf Version: 2024-02-01



#	Article	IF	CITATIONS
1	Assessment of GPS global ionosphere maps (GIM) by comparison between CODE GIM and TOPEX/Jason TEC data: Ionospheric perspective. Journal of Geophysical Research, 2010, 115, .	3.3	102
2	Characteristics of global plasmaspheric TEC in comparison with the ionosphere simultaneously observed by Jasonâ€1 satellite. Journal of Geophysical Research: Space Physics, 2013, 118, 935-946.	2.4	86
3	Densities and vibrational distribution of H ₃ ⁺ in the Jovian auroral ionosphere. Journal of Geophysical Research, 1992, 97, 6093-6101.	3.3	70
4	Chemistry of the Jovian auroral ionosphere. Journal of Geophysical Research, 1999, 104, 16541-16565.	3.3	65
5	A climatology of mediumâ€scale gravity wave activity in the midlatitude/lowâ€latitude daytime upper thermosphere as observed by CHAMP. Journal of Geophysical Research: Space Physics, 2014, 119, 2187-2196.	2.4	62
6	Globally nonsimultaneous Forbush decrease events and their implications. Journal of Geophysical Research, 2008, 113, .	3.3	44
7	Solar Cycle Variation of the Interplanetary Forward Shock Drivers Observed at 1ÂAU. Solar Physics, 2007, 245, 391-410.	2.5	38
8	The role of the vertical <l>E×<i><b& drift for the formation of the longitudinal plasma density structure in the low-latitude F region. Annales Geophysicae, 2008, 26, 2061-2067.</b& </i></l>	amp;gt;B&	amg;lt;/B&am
9	Seasonal variation of meteor decay times observed at King Sejong Station (62.22°S, 58.78°W), Antarctica. Journal of Atmospheric and Solar-Terrestrial Physics, 2010, 72, 883-889.	1.6	31
10	The Jovian ionospheric E region. Geophysical Research Letters, 1991, 18, 123-126.	4.0	30
11	Hydrocarbon ions in the lower ionosphere of Saturn. Journal of Geophysical Research: Space Physics, 2014, 119, 384-395.	2.4	29
12	Vertical structure of mediumâ€scale traveling ionospheric disturbances. Geophysical Research Letters, 2015, 42, 9156-9165.	4.0	28
13	An empirical model for prediction of geomagnetic storms using initially observed CME parameters at the Sun. Journal of Geophysical Research, 2010, 115, .	3.3	27
14	The effects of deionization processes on meteor radar diffusion coefficients below 90 km. Journal of Geophysical Research D: Atmospheres, 2014, 119, 10027-10043.	3.3	27
15	Magnetic signatures of mediumâ€scale traveling ionospheric disturbances as observed by CHAMP. Journal of Geophysical Research, 2009, 114, .	3.3	25
16	Mesospheric signatures observed during 2010 minor stratospheric warming at King Sejong Station (62°S, 59°W). Journal of Atmospheric and Solar-Terrestrial Physics, 2016, 140, 55-64.	1.6	25
17	Mesospheric temperature estimation from meteor decay times of weak and strong meteor trails. Journal of Atmospheric and Solar-Terrestrial Physics, 2012, 89, 18-26.	1.6	22
18	The effect of recombination and attachment on meteor radar diffusion coefficient profiles. Journal of Geophysical Research D: Atmospheres, 2013, 118, 3037-3043.	3.3	22

#	Article	IF	CITATIONS
19	New method of estimating temperatures near the mesopause region using meteor radar observations. Geophysical Research Letters, 2016, 43, 10,580.	4.0	22
20	High-Resolution Ultraviolet Spectroscopy of Jupiter's Aurora with the Hubble Space Telescope. Astrophysical Journal, 1995, 447, 906.	4.5	22
21	Seasonal variation of wave activities near the mesopause region observed at King Sejong Station (62.22°S, 58.78°W), Antarctica. Journal of Atmospheric and Solar-Terrestrial Physics, 2013, 105-106, 30-38.	1.6	21
22	Effect of Southern Hemisphere Sudden Stratospheric Warmings on Antarctica Mesospheric Tides: First Observational Study. Journal of Geophysical Research: Space Physics, 2018, 123, 2127-2140.	2.4	21
23	Assimilation of Multiple Data Types to a Regional Ionosphere Model With a 3Dâ€Var Algorithm (IDA4D). Space Weather, 2019, 17, 1018-1039.	3.7	18
24	Unusual Changes in the Antarctic Middle Atmosphere During the 2019 Warming in the Southern Hemisphere. Geophysical Research Letters, 2020, 47, e2020GL089199.	4.0	17
25	Tomography Reconstruction of Ionospheric Electron Density with Empirical Orthonormal Functions Using Korea GNSS Network. Journal of Astronomy and Space Sciences, 2017, 34, 7-17.	1.0	17
26	Do minor sudden stratospheric warmings in the Southern Hemisphere (SH) impact coupling between stratosphere and mesosphere–lower thermosphere (MLT) like major warmings?. Earth, Planets and Space, 2017, 69, .	2.5	15
27	The 4Dâ€var Estimation of North Korean Rocket Exhaust Emissions Into the Ionosphere. Journal of Geophysical Research: Space Physics, 2018, 123, 2315-2326.	2.4	15
28	On Imaging South African Regional Ionosphere Using 4Dâ€var Technique. Space Weather, 2019, 17, 1584-1604.	3.7	15
29	Forecasting the ionospheric F2 Parameters over Jeju Station (33.43°N, 126.30°E) by Using Long Short-Term Memory. Journal of the Korean Physical Society, 2020, 77, 1265-1273.	0.7	15
30	The Observation and SDâ€WACCM Simulation of Planetary Wave Activity in the Middle Atmosphere During the 2019 Southern Hemispheric Sudden Stratospheric Warming. Journal of Geophysical Research: Space Physics, 2021, 126, e2020JA029094.	2.4	15
31	Ground-based Observations for the Upper Atmosphere at King Sejong Station, Antarctica. Journal of Astronomy and Space Sciences, 2014, 31, 169-176.	1.0	15
32	First simultaneous multistation observations of the polar cap thermospheric winds. Journal of Geophysical Research: Space Physics, 2017, 122, 907-915.	2.4	13
33	Variation of the topside ionosphere during the last solar minimum period studied with multisatellite measurements of electron density and temperature. Journal of Geophysical Research: Space Physics, 2016, 121, 7269-7286.	2.4	12
34	Meteor radar observations of vertically propagating lowâ€frequency inertiaâ€gravity waves near the southern polar mesopause region. Journal of Geophysical Research: Space Physics, 2017, 122, 4777-4800.	2.4	12
35	Periodicity in the occurrence of equatorial plasma bubbles derived from the C/NOFS observations in 2008–2012. Journal of Geophysical Research: Space Physics, 2017, 122, 1137-1145.	2.4	12
36	Potential of Regional Ionosphere Prediction Using a Long Shortâ€Term Memory Deepâ€Learning Algorithm Specialized for Geomagnetic Storm Period. Space Weather, 2021, 19, e2021SW002741.	3.7	12

#	Article	IF	CITATIONS
37	Effects of the dipole tilt and northward and duskward IMF on dayside magnetic reconnection in a global MHD simulation. Journal of Geophysical Research, 2010, 115, .	3.3	11
38	Regional optimization of the IRI-2012 output (TEC, foF2) by using derived GPS-TEC. Journal of the Korean Physical Society, 2015, 66, 1599-1610.	0.7	11
39	Polar Thermospheric Winds and Temperature Observed by Fabryâ€Perot Interferometer at Jang Bogo Station, Antarctica. Journal of Geophysical Research: Space Physics, 2017, 122, 9685-9695.	2.4	11
40	Climatology of polar ionospheric density profile in comparison with mid-latitude ionosphere from long-term observations of incoherent scatter radars: A review. Journal of Atmospheric and Solar-Terrestrial Physics, 2020, 211, 105449.	1.6	11
41	Activities of Smallâ€6cale Gravity Waves in the Upper Mesosphere Observed From Meteor Radar at King Sejong Station, Antarctica (62.22°S, 58.78°W) and Their Potential Sources. Journal of Geophysical Research D: Atmospheres, 2021, 126, e2021JD034528.	3.3	11
42	Equatorial spreadFfound in 5577 Ã and 6300 Ã airglow observations from Hawaii. Journal of Geophysical Research, 2002, 107, SIA 6-1.	3.3	10
43	KASINICS: Near Infrared Camera System for the BOAO 1.8 m Telescope. Publication of the Astronomical Society of Japan, 2008, 60, 849-856.	2.5	10
44	Hot CH4 in the polar regions of Jupiter. Icarus, 2015, 257, 217-220.	2.5	10
45	Evaluation of estimated mesospheric temperatures from 11-year meteor radar datasets of King Sejong Station (62°S, 59°W) and Esrange (68°N, 21°E). Journal of Atmospheric and Solar-Terrestrial Physics, 2019, 196, 105148.	1.6	10
46	A climatology study on ionospheric F 2 peak over Anyang, Korea. Earth, Planets and Space, 2011, 63, 335-349.	2.5	9
47	A statistical study on the <i>F</i> ₂ layer vertical variation during nighttime mediumâ€scale traveling ionospheric disturbances. Journal of Geophysical Research: Space Physics, 2017, 122, 3586-3601.	2.4	9
48	Regional Ionospheric Parameter Estimation by Assimilating the LSTM Trained Results Into the SAMI2 Model. Space Weather, 2020, 18, e2020SW002590.	3.7	9
49	Characteristics of Ionospheric Irregularities Using GNSS Scintillation Indices Measured at Jang Bogo Station, Antarctica (74.62°S, 164.22°E). Space Weather, 2020, 18, e2020SW002536.	3.7	8
50	Spectral observations of FUV auroral arcs and comparison with invertedâ€V precipitating electrons. Journal of Geophysical Research, 2010, 115, .	3.3	7
51	Where does the plasmasphere begin? Revisit to topside ionospheric profiles in comparison with plasmaspheric TEC from Jason-1. Journal of Geophysical Research: Space Physics, 2016, 121, 10,091-10,102.	2.4	7
52	The Analysis of the Topside Additional Layer of Martian Ionosphere Using MARSIS/Mars Express Data. Journal of Astronomy and Space Sciences, 2012, 29, 337-342.	1.0	7
53	A Data Assimilated Regional Ionosphere Model Using the Total Electron Content from the Korean GPS Network. Journal of the Korean Physical Society, 2018, 72, 826-834.	0.7	6
54	Advanced meteor radar observations of mesospheric dynamics during 2017 minor SSW over the tropical region. Advances in Space Research, 2019, 64, 1940-1947.	2.6	6

#	Article	IF	CITATIONS
55	Simultaneous Observations of SAR Arc and Its Ionospheric Response at Subauroral Conjugate Points (LÂ≃Â2.5) During the St. Patrick's Day Storm in 2015. Journal of Geophysical Research: Space Physics, 2020, 125, e2019JA027321.	2.4	6
56	A Comparison of Fabry–Perot Interferometer and Meteor Radar Wind Measurements Near the Polar Mesopause Region. Journal of Geophysical Research: Space Physics, 2021, 126, e2020JA028802.	2.4	6
57	Reconstruction of the Regional Total Electron Content Maps Over the Korean Peninsula Using Deep Convolutional Generative Adversarial Network and Poisson Blending. Space Weather, 2022, 20, .	3.7	6
58	EISCAT Observation of Waveâ€Like Fluctuations in Vertical Velocity of Polar Mesospheric Summer Echoes Associated With a Geomagnetic Disturbance. Journal of Geophysical Research: Space Physics, 2018, 123, 5182-5194.	2.4	5
59	Gravity Wave Investigations over Comandante Ferraz Antarctic Station in 2017: General Characteristics, Wind Filtering and Case Study. Atmosphere, 2020, 11, 880.	2.3	5
60	Temperature teleâ€connections between the tropical and polar middle atmosphere in the Southern Hemisphere during the 2010 minor sudden stratospheric warming. Atmospheric Science Letters, 2021, 22, e1010.	1.9	5
61	Unusual Enhancements of NmF2 in Anyang Ionosonde Data. Journal of Astronomy and Space Sciences, 2013, 30, 223-230.	1.0	5
62	Mapping the East African Ionosphere Using Ground-based GPS TEC Measurements. Journal of Astronomy and Space Sciences, 2016, 33, 29-36.	1.0	5
63	Jovian aurorae. Reports on Progress in Physics, 1998, 61, 525-568.	20.1	4
64	Paleoclimate Signals of Lake Hovsgol, Mongolia, Over the Last 19,000 Years Using Authigenic Beryllium Isotopes. Radiocarbon, 2014, 56, 1139-1150.	1.8	4
65	Long-term trend of mesospheric temperatures over Kiruna (68°N, 21°E) during 2003–2014. Journal of Atmospheric and Solar-Terrestrial Physics, 2017, 161, 83-87.	1.6	4
66	Observation of a persistent Leonid meteor train with an all-sky camera. Journal of Atmospheric and Solar-Terrestrial Physics, 2004, 66, 1001-1009.	1.6	3
67	Development of a data-verified ionospheric model with an ionosonde network. Journal of the Korean Physical Society, 2016, 68, 1359-1370.	0.7	3
68	A case study of convectively generated gravity waves coupling of the lower atmosphere and mesosphere-lower thermosphere (MLT) over the tropical region: An observational evidence. Journal of Atmospheric and Solar-Terrestrial Physics, 2018, 169, 45-51.	1.6	3
69	Regional ionosphere specification by assimilating ionosonde data into the SAMI2 model. Advances in Space Research, 2019, 64, 1343-1357.	2.6	3
70	Observations of ionospheric irregularities and its correspondence with sporadic e occurrence over South Korea and Japan. Advances in Space Research, 2021, 67, 2207-2218.	2.6	3
71	Detection of an Impact Flash Candidate on the Moon with an Educational Telescope System. Journal of Astronomy and Space Sciences, 2015, 32, 121-125.	1.0	3
72	A regional ionospheric assimilation study with GPS and COSMIC measurements using a 3D-var algorithm (IDA4D). Advances in Space Research, 2022, 69, 2489-2500.	2.6	3

#	Article	IF	CITATIONS
73	Molecular emissions from the atmospheres of giant planets and comets: Needs for spectroscopic and collision data. Advances in Atomic, Molecular and Optical Physics, 2001, , 129-162.	2.3	2
74	Reconstruction of Plasmaspheric Density Distributions by Applying a Tomography Technique to Jason‹ Plasmaspheric TEC Measurements. Radio Science, 2018, 53, 866-873.	1.6	2
75	Low-latitude mesospheric signatures observed during the 2017 sudden stratospheric warming using the fuke meteor radar and ERA-5. Journal of Atmospheric and Solar-Terrestrial Physics, 2020, 207, 105352.	1.6	2
76	Dynamically Unstable Strong Wind Shears Observed in the Polar Mesosphere Summer Echo Layer Associated With Geomagnetic Disturbances. Journal of Geophysical Research: Space Physics, 2020, 125, e2019JA027013.	2.4	2
77	Basic Lunar Topography and Geology for Space Scientists. Uju Gisulgwa Eungyong, 2021, 1, 217-240.	0.3	2
78	Mesospheric Temperatures over Apache Point Observatory (32°N, 105°W) Derived from Sloan Digital Sky Survey Spectra. Journal of Astronomy and Space Sciences, 2017, 34, 119-125.	1.0	2
79	Investigation of Reflectance Distribution and Trend for the Double Ray Located in the Northwest of Tycho Crater. Journal of Astronomy and Space Sciences, 2015, 32, 161-166.	1.0	2
80	Ionospheric Density Oscillations Associated With Recurrent Prompt Penetration Electric Fields During the Space Weather Event of 4 November 2021 Over the Eastâ€Asian Sector. Journal of Geophysical Research: Space Physics, 2022, 127, .	2.4	2
81	High-Resolution Optical and Infrared Observations of Molecules in Comets. Symposium - International Astronomical Union, 2000, 197, 471-480.	0.1	1
82	A comparison of FUV dayglows measured by STSAT-1/FIMS with the AURIC model in a geomagnetic quiet condition. Journal of the Korean Physical Society, 2014, 65, 786-791.	0.7	1
83	Anisotropic diffusion of meteor trails due to the geomagnetic field over King Sejong Station (62.2°S,) Tj ETQq1 1	0.78431 1.4	4 rgBT /Ove
84	Manually scaling ionograms measured by Icheon and Jeju ionosondes over a 2-year period (2017–2018). Journal of the Korean Physical Society, 2021, 78, 1249-1265.	0.7	1
85	Modeling total electron content derived from radio occultation measurements by COSMIC satellites over the African region. Annales Geophysicae, 2020, 38, 1203-1215.	1.6	1
86	A Modeling Analysis of the Apparent Linear Relation Between Mesospheric Temperatures and Meteor Height Distributions Measured by a Meteor Radar. Journal of Geophysical Research: Space Physics, 2022, 127, .	2.4	1
87	Mesospheric Shortâ€Period Gravity Waves in the Antarctic Peninsula Observed in All‣ky Airglow Images and Their Possible Source Locations. Journal of Geophysical Research D: Atmospheres, 2021, 126, .	3.3	1
88	Observation of a persistent Leonid meteor train with an all-sky camera. Journal of Atmospheric and Solar-Terrestrial Physics, 2004, 66, 1001-1001.	1.6	0
89	High-latitude mesospheric intense turbulence associated with high-speed solar wind streams. Astrophysics and Space Science, 2019, 364, 1.	1.4	0
90	Characterizing ionospheric disturbances caused by the North Korean rocket (Hwasung-15) using a four-dimensional variational (4D-VAR) data-assimilation model. Journal of the Korean Physical Society, 0, , 1.	0.7	0

#	Article	IF	CITATIONS
91	Inferring the Horizontal Speed of an Ionospheric Irregularity from a Single GPS Scintillation Receiver at High Latitudes. Journal of Geophysical Research: Space Physics, 2021, 126, e2021JA029277.	2.4	0
92	Verifications of a 3-D regional ionospheric physics-based model over the Korean peninsula. Advances in Space Research, 2022, 69, 1257-1271.	2.6	0